

STRUCTURAL, OPTICAL AND ELECTRICAL PROPERTIES OF CuSbS₂ THESE AMORPHOUS FILMS: EFFECT OF THE THICKNESS VARIATION

A. RABHI*, M. KANZARI

Laboratoire de Photovoltaïque et Matériaux Semi-conducteurs-ENIT BP 37, Le belvédère 1002, Tunis, Tunisia

Chalcostibite CuSbS₂ thin films have been deposited on no heated glass substrates by single source vacuum evaporation method. The pressure during evaporation was maintained at 10⁻⁵ Torr. All the as-deposited films were amorphous. The structural, optical and electrical properties have been investigated relating the thickness variation. The optical properties revealed the presence of direct band gaps with energies in the 1.36 to 2.21 eV range. Absorption coefficients higher than 10⁵ cm⁻¹ were found. The X-ray diffraction analysis show an improvement in the crystallinity of the films as thickness values increases. Secondary phases are observed corresponding to the Sb₂S₃. The electrical conductivity of the CuSbS₂ thin film is in order 10⁻⁵ Ω⁻¹ cm⁻¹. Hot probe testing indicated that this is p-type. So, the absorber material is a good candidate for photovoltaic applications.

(Received May 5, 2011; Accepted June 17, 2011)

Keywords: CuSbS₂, Amorphous films, Weight of powder, Thickness variation, Structural properties, Optical properties, Electrical properties.

1. Introduction

The ternary chalcogenide CuSbS₂ compound is one of the important semiconductors with narrow band gap showing potential applications in various optoelectronic devices such as infrared detectors and solar cells [1]. However, The sulfosalt compound, CuSbS₂ may be the most photovoltaic p-i-n structure promising absorber materials for three-dimensional (3D) films solar cells [2] having a high coefficient and band gap of 1.5 eV [3] being close to the optimum range for photovoltaic conversion [4]. The sulfosalt compound CuSbS₂ is an inorganic absorber material [5], it is stable and non-toxic. Several methods of depositing CuSbS₂ polycrystalline thin films, evaporation [6], chemical vapor deposition CVD, sputtering, and spray pyrolysis [3], chemical bath deposition (CBD) [7] have been investigated. This paper deals with the effects of increasing thickness on the structural, optical and electrical properties of amorphous CuSbS₂ thin films.

2. Experimental details

2.1 Film preparation

The CuSbS₂ thin films are carried out from a solid solution containing copper, antimony and sulphur. Stoichiometric amounts of the elements of 99.999% purity Cu, Sb and S were used to prepare the initial ingot of CuSbS₂. CuSbS₂ thin films were prepared by the evaporation of the CuSbS₂ powder in a high-vacuum system with a base pressure of 10⁻⁵ Torr. Crushed powder of this ingot was used as raw material for the thermal evaporation and a molybdenum crucible (resistivity heated) was used as evaporator. Corning 7059 glasses substrates were used. The as-

*Corresponding author: adel_rabhi@yahoo.fr

deposited films thicknesses were in the range of 70–368 nm. The films were prepared in vacuum atmosphere in ambient temperature 25°C.

2.2 Characterization of the deposited CuSbS₂

The structure of the CuSbS₂ thin films was determined by means of X-ray diffraction (XRD) using a D8 Advance diffractometer with CuK α radiation ($\lambda=1.5418$ Å). Transmission and reflection spectra were measured at normal incidence in the wavelength range 300–1800 nm. The films thicknesses were calculated from the positions of the interference maxima and minima of reflection spectra using a standard method [8]. The as-deposited films thicknesses were in the range of 70–368 nm corresponding to the initial weight powder 0.01-0.09g respectively. The absorption coefficients were deduced from Transmission and reflection spectra's [9]. The measurements of surface roughness were determined by an optical method. The hot probe method measurements were carried out in order to determine the conduction types of the samples.

3. Results and discussion

3.1. Thickness Variation

Fig. 1 shows the thickness of the CuSbS₂ thin films obtained at different weights of powder. Figure (1) shows an increase linear behavior of a variation of the thickness with the weight of powder.

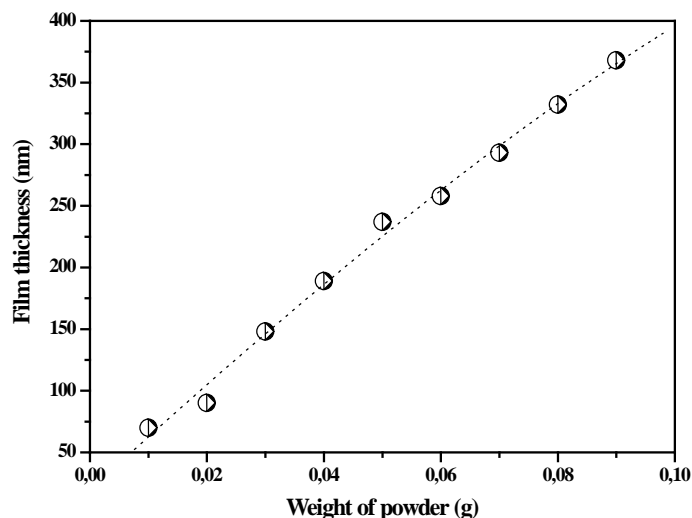


Fig. 1: Values of thickness as function of variation a weight powder.

3.2. Structural properties

Fig. 2 shows the results of our XRD measurements of the as-deposited CuSbS₂ thin films. The presence of identifiable peaks in the diffractograms suggests that the films are not amorphous but crystalline in nature [10]. It is clear, to state the important role of temperature in the films crystallization. The pattern for the film displayed diffraction peaks at 2θ values of approximately 12.80°, 19.75°, 23.73°, 29.42° and 31.63° which corresponding to (002), (102), (103), (200) and (400) planes respectively (JCPDS 65-2416). It may be noted that a secondary phase with peaks assigned to (202), (111) and (006) planes appears which attributed to the Sb₂S₃ material (JCPDS 74-1046). In addition, we note that an increase in film thicknesses leads to an improvement in the crystallinity of the CuSbS₂ film [7, 11].

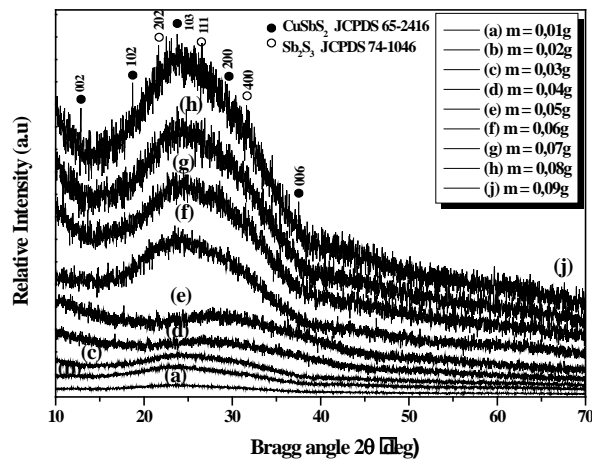


Fig. 2: X-ray diffraction spectra of CuSbS_2 thin films as-deposited at different weight of powder.

From the relationship between crystal grain size and X-ray line broadening, described by Scherer's equation $D = \frac{0.9\lambda}{\beta \cos \theta}$ (D = average crystallite dimension, λ is the X-ray wavelength, β = the full-width at half-maximum (FWHM), and θ the Bragg angle [12]). The average grain size was estimated to be 18 nm of the CuSbS_2 film.

3.3. Optical properties

3.3.1. Transmission and reflection spectra

The transmission and reflection spectra in the wavelength range 300–1800 nm at normal incidence of the as-deposited CuSbS_2 thin films are shown respectively in Figs. 3, 4a and 4b. The averages of the transmission and the reflection values of all the layers in the transparency region (600 - 1800 nm) are 60% and 30 % respectively.

The transmission and the reflection spectra's show interference patterns with sharp fall of the transmission at the band edge, which is an indication of good homogeneity of the films.

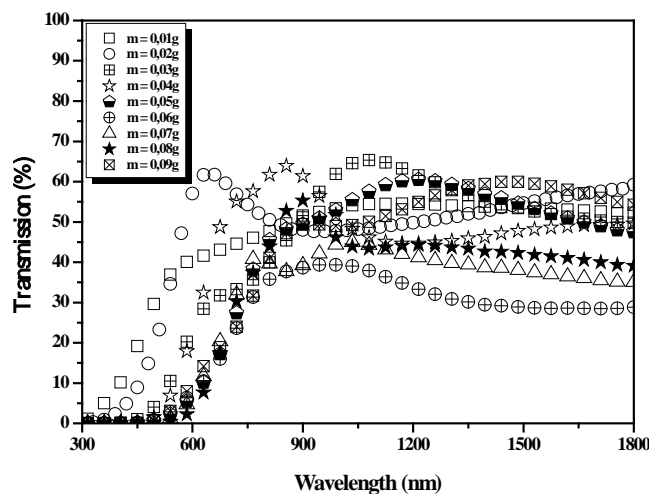
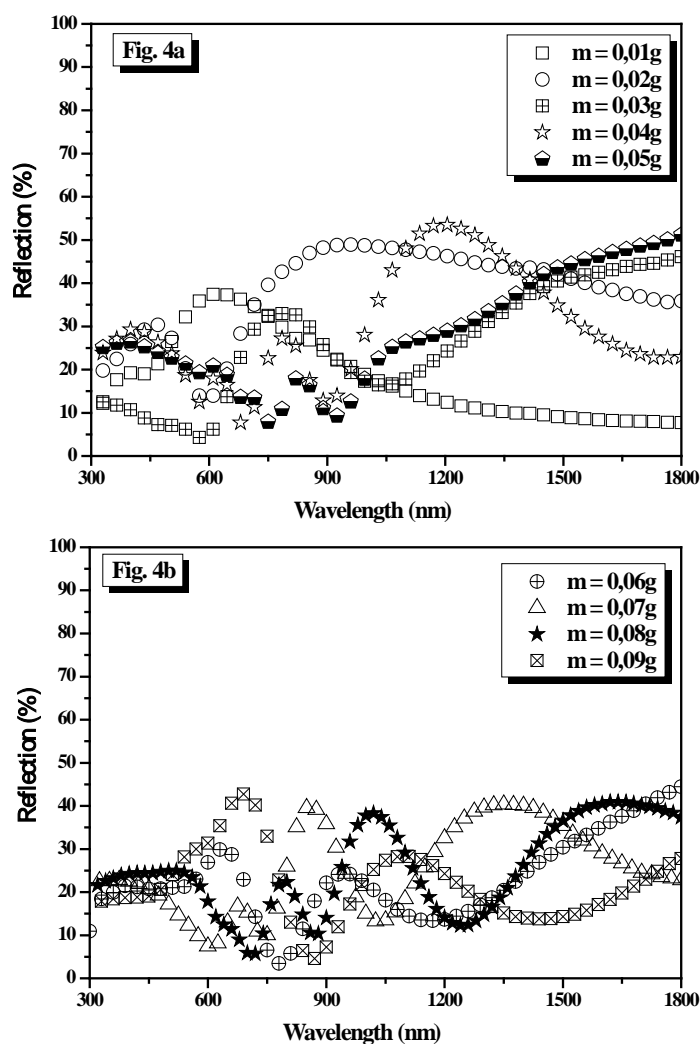


Fig. 3: Optical transmission spectra of CuSbS_2 thin films as-deposited at different weight of powder.



Figs. 4a and 4b: Optical reflection spectra of CuSbS₂ thin films as-deposited at different weight of powder.

3.3.2. Absorption coefficients and energy gap

To calculate the absorption coefficient α ($h\nu$), the following relation was used [13, 14]:

$$\alpha = \frac{1}{d} \cdot \ln\left[\frac{(1-R)^2}{T}\right] \quad (1)$$

where: d is the thickness of thin film, R and T are the reflection and the transmission coefficients respectively. Fig. 5 shows the absorption coefficients versus the photon energy for the as-deposited films at different thickness variation.

It can be seen that all the films have relatively high absorption coefficients between 10^5 cm^{-1} and 10^6 cm^{-1} in the visible and near-IR spectral range. This result is very important because we know that the spectral dependence of the absorption coefficient affects the solar conversion efficiency [15]. It is now well established that CuSbS₂ is a direct gap semiconductor [16, 17]. The absorption coefficient α is related to the energy gap according to the following equation [18]:

$$(\alpha h\nu)^2 = A(h\nu - E_g) \quad (2)$$

where A is a constant, h is the Planck constant. The values of direct optical transition are shown in Fig. 6. The direct band gap energy stabilises between 1,5 eV and 1,8 eV with increasing the film thickness (Fig. 7).

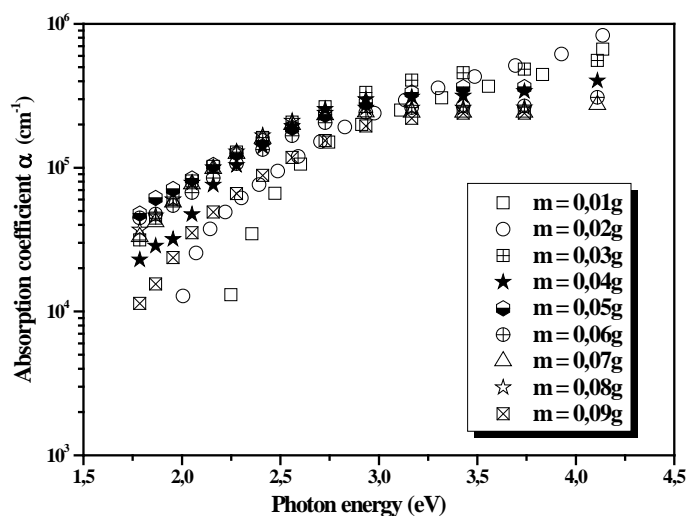


Fig. 5: Absorption coefficients of CuSbS_2 thin films as-deposited at different thickness.

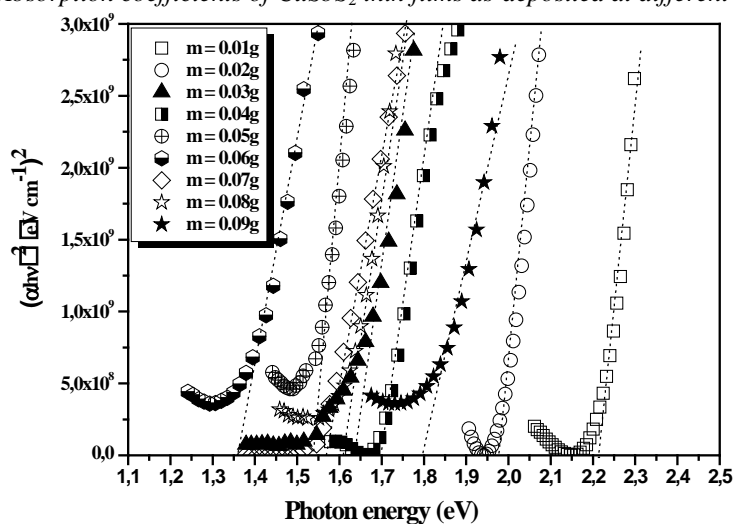


Fig. 6: Plots of $(\alpha h\nu)^2$ versus $h\nu$ for the CuSbS_2 thin films as-deposited at different thickness.

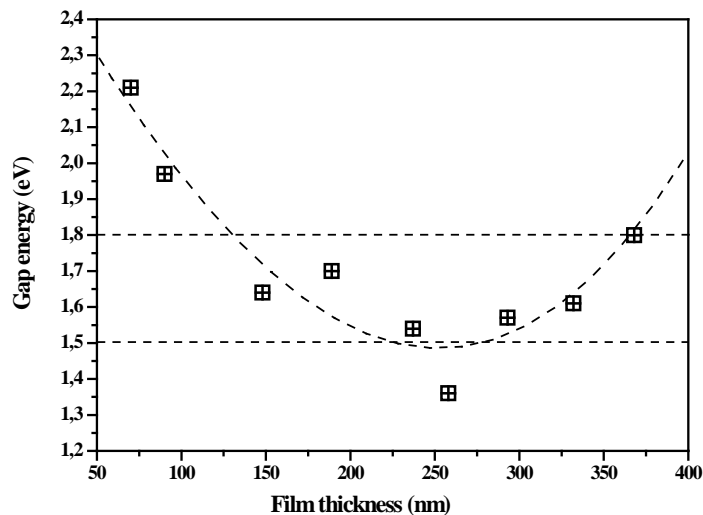


Fig. 7: Energy gap of CuSbS_2 thin films as-deposited at different thickness.

3.3.3. Measurements of surface roughness

For reflection from a rough surface the reflection coefficient R_s of light reflected in a specular direction from a surface which has a gaussian distribution of the heights of its irregularities may be written as [19, 20].

$$\frac{R_s}{R_t} = \exp\left[-\left(\frac{4\pi\sigma}{\lambda}\right)^2\right] + \left[1 - \exp\left[-\left(\frac{4\pi\sigma}{\lambda}\right)^2\right]\right] \times \left[1 - \exp\left[-\left(\frac{\beta\pi\sigma}{u\lambda}\right)^2\right]\right] \quad (3)$$

Where R_s is the reflection from a perfectly smooth surface, σ and u are the r.m.s height and r.m.s slope of the irregularities in the surface, respectively, λ is the wavelength of the incident radiation and β is the half acceptance angle of the instrument. R_t may be taken to be equal to $R_s + R_{\text{diff}}$, with R_{diff} being the diffused part of the reflectance. The first term on the righthand side of equation (3) describes the coherent part of the reflectance, while the second term describes the incoherently reflected light, as recorded by the spectrophotometer. If is small, the incoherent term can be neglected, and we may write:

$$\ln\left(\frac{R_s}{R_t}\right) = -\frac{(4\pi\sigma)^2}{\lambda^2} + C \quad (4)$$

Where C is a constant arising from the spatial fluctuations of the optical constants.

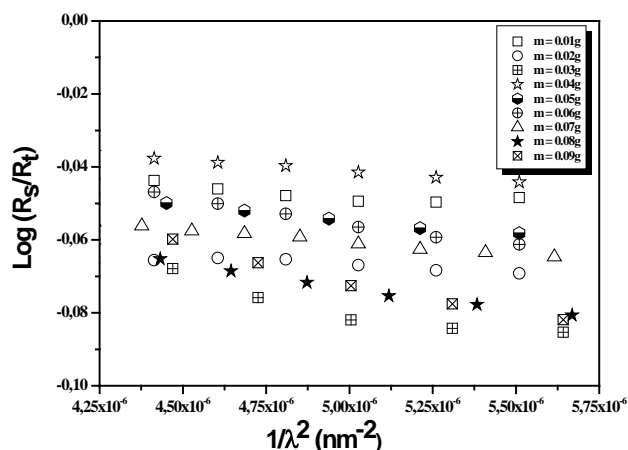


Fig. 8: Plots of $\text{Log}(R_s/R_t)$ versus $(1/\lambda^2)$ for the CuSbS_2 thin films as-deposited at different thickness.

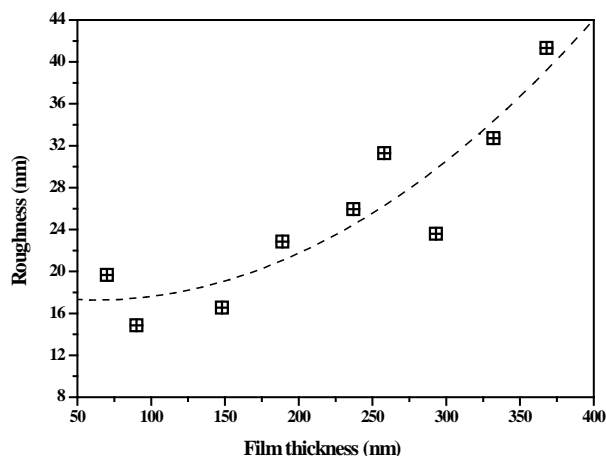


Fig. 9: Surface roughness of CuSbS_2 thin films as-deposited at different thickness.

Thus the slope of $\ln(R_s/R_t)$ versus $(1/\lambda^2)$ will give the surface roughness of the film (Fig.8).

The roughness values evaluated in this way for the CuSbS_2 films were indicated in Fig. 9. We note an increase in the roughness values with increasing the films thicknesses.

3.3.4. Extinction coefficient k

Fig. 10 shows the extinction coefficient k for the as-deposited CuSbS_2 thin films as a function of wavelength. It is obvious that a decrease in the k values is clearly observed in the part of the visible spectral range. The extinction coefficient, k , is found to decrease with increase in wavelength of the incident photon. Indeed, for the thickness below 100 nm the coefficient, k , tends to be zero in the visible spectral range. It may be noted that from the thickness values 150 nm the coefficient, k , tends to be zero in the near-IR spectral range. The transparency of amorphous CuSbS_2 thin films decreases when the thickness increases. These results were well correlated with the surface roughness values.

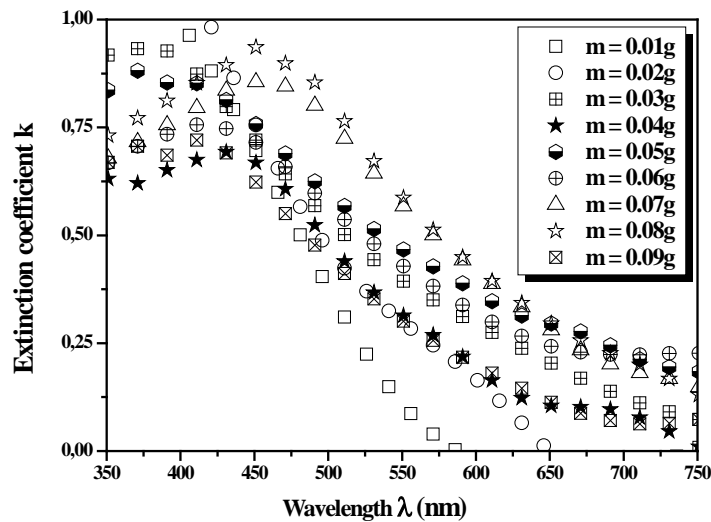


Fig. 10: Variation of the extinction coefficient of CuSbS_2 thin films as-deposited at different thickness.

3.4. Electrical properties

The electrical conductivity of CuSbS_2 films is in the range of $3 \cdot 10^{-5} - 6 \cdot 10^{-5} \Omega^{-1} \text{cm}^{-1}$. For a polycrystalline thin film, the electrical conductivity has to be still higher. The electrical conductivity of the mineral sample has been reported to be $2 \cdot 10^{-4} \Omega^{-1} \text{cm}^{-1}$ (p-type) with a room temperature [21]. No important significant effects on the electrical properties of CuSbS_2 films with different thicknesses ranging from 70 to 368 nm. In all cases the samples revealed p-type conductivity.

4. Conclusions

We have qualitatively evaluated the effect of thickness on structural, optical and electrical properties of CuSbS_2 thin films deposited by single source on no heated glass substrates. However, all the films and independently of the thickness were amorphous. The surface roughness is found to increase with increasing film thickness. Absorption coefficients higher than 10^5cm^{-1} were found. For the CuSbS_2 films, the thickness has light effects on the electrical properties. The phenomenon is attributed to exclusion of grain boundary scattering limiting the electrical transport of the electrons.

References

- [1] J. Zhou, G. Bian, Q. Zhu, Y. Zhang, C. Li, J. Dai, Solvothermal crystal growth of CuSbQ_2 (Q = S, Se) and the correlation between macroscopic morphology and microscopic structure, *Journal of Solid State Chemistry* **182**, 259 (2009).
- [2] Simona Manolache, Anca Duta, Luminita Isac, Marian Nanu, Albert Goossens, Joop Schoonman, *Thin Solid Films* **515**, 5957 (2007).
- [3] Y.R. Lazcano, M.T.S. Nair, P.K. Nair, *J. Cryst. Growth* **223**, 399 (2001).
- [4] J. Nelson, *the Physics of Solar Cells*, Imperial College Press, 2003.
- [5] V.P. Zhuze, V.M. Sergeeva, E.L. Shteum, *Soviet Phys. Techn. Phys.* **3**, 1925 (1958).
- [6] Leila I. Soliman, Aziza M. Abo EL Soad, Hamida A. Zayed, Sammer A. EL Ghfar, *Fizika* **A11-4**, 139 (2002).
- [7] S. C. Ezugwu, F. I. Ezema, P. U. Asogwa, *Chalcogenide Letters* **7**, 369 (2010).
- [8] L. Vriens, W. Rippens, *Appl. Opt.* **22**, 4105 (1983).
- [9] A. Rabhi, M. Kanzari, B. Rezig, *Materials Letters* **62**, 3576 (2008).
- [10] P.U. Asogwa, Ph.D, *the Pacific Journal of Science and Technology* **10** (2009).
- [11] S.C. Ezugwu, F.I. Ezema, R.U.Osuji, P.U. Asogwa, A.B.C. Ekwealor and B.A. Ezekoye, *Optoelectron. Adv. Mater.-Rapid Comm.* **3**, 141 (2009).
- [12] V.K. Gandotra, K.V. Ferdinand, C. Jagadish, A. Kumar, P.C. Mathur, *Phys. Stat. Sol. A* **98**, 595 (1986).
- [13] D.E. Milovzorov, A.M. Ali, T. Inkuma, Y. Kurata, T. Suzuki, S. Hasegawa, *Thin Solid Films* **382**, 47 (2001).
- [14] T.M. Wang, S.K. Zheng, W.C. Hao, C. Wang, *Surf. Coat. Technol.* **155**, 141 (2002).
- [15] S. C. Ezugwu, F. I. Ezema, P. U. Asogwa, *Chalcogenide Letters* **7**, 341 (2010).
- [16] M.T.S. Nair, Y. Rodríguez-Lazcano, Y. Peña, S. Messina, J. Campos, P.K. Nair, *Mater. Res. Soc. Symp. Proc. Materials Research Society* **836**, 37 (2005).
- [17] Y. Rodríguez-Lazcano, M.T.S. Nair, P.K. Nair, *J. Electrochem. Soc.* **152**(8) 635 (2005).
- [18] N.F. Mott, E.A. Davis, *Electronic processes in Non-Crystalline Materials*, Clarendon Press, Oxford, 1971.
- [19] Elsevier sequoia S.A, Lausanne-Printed in the Netherlands. *Thin Solid Film* **46**, 127 (1977).
- [20] M. Kanzari and B. Rezig, *Semicond. Sci. Technol.* **15**, 335 (2000).
- [21] I. Grigas, N. N. Mozgova, A. Orlyukas, V. Samulenis, *Sov. Phys. Crystallogr.* **20**, 741 (1976).